Fachtagung "Experimentelle Strömungsmechanik"
6. – 8. September 2016, Cottbus

Komplementäre experimentelle und numerische Untersuchung der Strömung über eine starre und eine flexible Halbkugel in turbulenter Strömung: Teil II: Numerische Simulationen

Complementary Experimental-Numerical Investigation of the Flow past a Rigid and a Flexible Hemisphere in Turbulent Flow: Part II: Numerical Simulations

M. Breuer, G. De Nayer, J.N. Wood
Professur für Strömungsmechanik, Helmut-Schmidt-Universität Hamburg, Germany

Fluid-Struktur-Interaktion; Halbkugelumströmung; Flexible Membran; Large-Eddy Simulation
Fluid-structure interaction; Flow past hemisphere; flexible membrane; large-eddy simulation

Abstract

The objective of the present contribution is a complementary investigation on the flow past a wall-mounted hemisphere exposed to a thick turbulent boundary layer. In a first step the flow around a rigid hemispherical obstacle is tackled by detailed wind tunnel measurements based on LDA and wall-resolved large-eddy simulations taking the oncoming turbulence into account. The close agreement found between the measurements and the predictions provides confidence to progress towards the objective to study the coupled fluid-structure interaction problem of a membranous lightweight structure air-inflated in a hemispherical shape and exposed to the same turbulent flow. The strategy of complementary experimental and numerical investigations is continued. **Part I** of the contribution reports about the measurements, whereas the present **part II** emphasizes on the numerical simulations of the flow around the rigid and flexible structure.

Introduction

The long-term objective of the present study is to investigate coupled fluid-structure interaction (FSI) problems of flexible thin-walled membranous structures exposed to turbulent flow fields. Technical applications are tents, awnings or air-inflated structures to mention only a few. As a typical example the flow around a surface-mounted hemispherical structure within a turbulent boundary layer appearing in various environmental and civil engineering applications is considered. The investigation relies on a complementary study taking detailed experimental wind tunnel measurements of the flow and the deformation of the structure (**part I**) and numerical simulations based on large-eddy simulations. In case of the air-inflated structure a partitioned FSI algorithm is taken into account to couple the fluid and the structure.
In a first step, the hemispherical structure is assumed to be rigid. The complex flow field arising around the wall-mounted hemisphere exposed to a turbulent boundary layer is predicted by highly resolved large-eddy simulations and analyzed at Re = 50,000 (Wood et al., 2016). Special emphasis is put on the generation of appropriate inflow conditions mimicking the influence of a fully developed thick turbulent boundary layer. For this purpose, the digital filter concept by Klein et al. (2003) is extended and used as a source term formulation inside the flow domain (Schmidt and Breuer, 2016). An analysis of the flow characteristics such as vortex shedding, the horseshoe vortex system and the recirculation area is carried out.

Karlsruhe, Germany, ISBN 978-3-9816764-2-6

In the second step, the rigid hemisphere is replaced by a flexible membranous structure. The coupled fluid-structure interaction is simulated based on the partitioned semi-implicit predictor-corrector coupling scheme especially developed for FSI applications within large-eddy simulations (Breuer et al., 2012). This scheme was thoroughly validated based on previous FSI benchmark cases particularly for turbulent flows (De Nayer et al., 2014; De Nayer and Breuer, 2014). The present paper includes comparisons between the predicted results and the measurements for the rigid hemisphere and first results for the coupled FSI problem.

Test Case Description

The investigated either rigid or flexible hemispherical body (diameter D) is mounted on a uniform wall. The structure is put into a thick turbulent boundary layer inside a wind tunnel, where the time-averaged flow is described by a 1/7 power law. At a distance of 1.5 diameters upstream of the bluff body the thickness of the boundary layer δ corresponds to the height of the hemisphere ($\delta = D/2$). Its characteristics are outlined in Wood et al. (2016). The Reynolds number of the air flow ($\rho_{air} = 1.225$ kg/m^3, $\mu_{air} = 18.27 \times 10^{-6}$ kg/(m s) at T = 20° C) is set to $Re = \rho_{air} D U_\infty / \mu_{air} = 50{,}000$. U_∞ is the undisturbed free-stream mean velocity in x-direction at standard atmospheric conditions. The flow is assumed to be incompressible and isotherm. For the flexible hemisphere an air-inflated thin membranous structure of hemispherical shape is used (Young's modulus $E_{silicone} = 7 \times 10^5$ Pa, Poisson's ratio $\nu_{silicone} = 0.49$, density $\rho_{silicone} = 1050$ kg/m^3, thickness $t = 1.6 \times 10^{-4}$ m). To reach the desired shape of a hemisphere the thin-walled membranous structure has to be air-inflated with an inner pressure difference of 44.2 Pa leading to a pre-stress $n_{membrane} = 7794.5$ Pa in the material. In order to observe visible structural deformations due to the wind load and to avoid wrinkles, this inner pressure difference is reduced to a value of $\Delta p_{FSI} = 19$ Pa in the present study.

Computational Methodology

The numerical method used relies on an efficient partitioned coupling scheme developed for dynamic FSI problems in turbulent flows (Breuer et al., 2012). Only a brief summary is presented here. The FSI code is based on two highly advanced solvers, one for the computational fluid dynamics (CFD) problem and one for the computational structural dynamics (CSD) problem. Between both a coupling program does the required exchange of data.
The fluid solver is an enhanced version of the in-house finite-volume code FASTEST-3D. It is based on a predictor-corrector scheme (projection method) of second-order accuracy in space and time: The momentum equations are advanced in time by an explicit three substeps low-storage Runge-Kutta scheme (predictor step). The predicted velocities are then updated during the correction step, which is based on the solution of a Poisson equation for the pressure correction also updating the pressure. At the end the velocities fulfill the mass conservation equation with a predefined accuracy. The equations are discretized on a curvilinear, block-structured body-fitted grid with a collocated variable arrangement. The midpoint rule is applied to approximate the surface and volume integrals with second-order accuracy. Furthermore, the flow variables are linearly interpolated to the cell faces leading to a second-order accurate central scheme. The coupling of the pressure and velocity fields on non-staggered grids is assured by the momentum interpolation technique of Rhie and Chow (1983). Turbulence is taken into account by the LES technique (Breuer, 2002): The large scales in the turbulent flow field are resolved directly, whereas the small scales are modeled either by the Smagorinsky (1963) model, its dynamic version or the WALE model. Owing to the moderate Reynolds number considered and the fine grid applied, the SGS model is found to have a limited influence on the results and thus the Smagorinsky model with $C_S = 0.1$ and van Driest damping near walls is appropriate.
In the context of FSI the classical Navier-Stokes equations formulated for a fixed domain have to be extended in order to take the deformation of the structure into account. In FASTEST-3D the grid fits to the body. Therefore, the Arbitrary Lagrangian-Eulerian (ALE)

Karlsruhe, Germany, ISBN 978-3-9816764-2-6

formulation is used. The remeshing method is performed algebraically by a combination of linear and transfinite interpolations.
The structure solver is the finite-element code Carat++ (Bletzinger et al., 2006; Fischer et al., 2010). This program was developed especially for the prediction of shell or membrane behavior and is based on advanced solution strategies for form finding and non-linear dynamic problems. The momentum equation written in a Lagrangian frame of reference is applied to describe the dynamic equilibrium of the structure. A constitutive relation providing a link between stress and strain is required to close the momentum equation. A St. Venant-Kirchhoff material law expressed by a second Piola-Kirchhoff stress tensor is assumed. For the time integration the implicit Newmark method is used.
To preserve the advantages of the highly adapted CFD and CSD codes and to realize an effective coupling algorithm, a partitioned but nevertheless strong coupling approach is chosen (Breuer et al., 2012). Since LES typically requires small time steps to resolve the turbulent flow field, the coupling scheme relies on the explicit predictor-corrector scheme forming the kernel of the fluid solver. The code coupling tool used is EMPIRE (Sicklinger et al., 2014) does the mapping between non-matching grids and the data exchange. For FSI cases the fluid forces and the structural displacements are sent from one solver to the other one. In the present investigation the consistent simple Mortar mapping method of Wang et al. (2016) is applied. It guarantees a correct exchange of the fluid stresses and the structural displacements from one solver to the other. The FSI coupling is carried out with a FSI convergence criterion set to $\varepsilon_{FSI} = 10^{-4}$. This criterion is for the L^2 norm of the displacement differences between two FSI subiterations and normalized by the displacement differences between the current and the old time step. To stabilize the simulation, a constant underrelaxation factor $\omega = 0.3$ is applied for the displacements during the FSI subiterations. To reach the FSI convergence faster, a linear extrapolation of the FSI interface displacements is carried out at the beginning of each time step (Breuer et al., 2012). Due to the small time step and consequently the small deformations between two time steps, only 5 FSI subiterations are typically required for the above setup.
The application of appropriate temporally and spatially correlated velocity distributions as inlet boundary conditions is essential to mimic the real oncoming turbulent boundary layer in the experiment. Therefore, a synthetic turbulence inflow generator (STIG) based on the digital filter concept of Klein et al. (2003) provides instantaneous three-dimensional velocities relying solely on the definition of one integral time scale (here: $T_{STIG}\, U_\infty/D = 2.79 \times 10^{-2}$), two integral length scales (here: $L_{STIG}/D = 2.06 \times 10^{-2}$) and the distributions of the mean velocity and Reynolds stresses taken from Wood et al. (2016). In order to avoid that the imposed turbulent flow field is damped out due to numerical diffusion in the coarsely resolved inflow region, a source term formulation developed by Schmidt and Breuer (2016) is applied. It allows to superimpose the synthetically generated turbulence upstream of the bluff body within the computational domain (x/D = -1.5) and thus in a finer resolved flow region.
In the present case a block-structured medium grid consisting of about 4.3 million control volumes (CVs) is used for the fluid flow. That differs from the fine reference grid used in Wood et al. (2016) which contained 30.72 million CVs. Similar to the fine grid the viscous sublayer is fully resolved and the first cell center is approximately located at a distance of $\Delta z/D = 5 \times 10^{-5}$ from the wall. The reduction is necessary in order to carry out the coupled FSI simulations within reasonable times. However, due to the high grid quality leading for example to averaged z^+ values (wall-normal direction) on the wall below 0.25 even on the medium grid, a close agreement was found for the results obtained on the medium and the fine grid in a preliminary study.
The structure is represented by a FEM grid containing 3784 triangular elements for 1943 nodes. All nodes have 6 degrees of freedom except the ones at z/D = 0. These bottom nodes cannot move in any translational direction due to the fact that the membranous structure is attached to the bottom wall. The small pressure difference $\Delta p_{FSI} = 19$ Pa between the interior and the surrounding and the pre-stress of the membrane $n_{membrane} = 7794.5$ Pa are prescribed in the CSD solver. The gravitational acceleration $g = 9.81$ m/s^2 is also taken into account in the CSD solver as a dead load acting on the volume of each element.

Karlsruhe, Germany, ISBN 978-3-9816764-2-6

Comparison of the Predictions and Measurements for the Rigid Hemisphere

In a first step of the evaluation the simulation results are compared with the LDA measurements of Wood et al. (2016) for the rigid hemisphere (see also **part I** of this contribution and Wood and Breuer, 2015). The unsteady flow patterns past a hemisphere can be classified into several regions (Savory and Toy, 1986). The hemispherical bluff body acts as an obstacle which leads to a positive pressure gradient so that the boundary layer separates from the ground forming the horseshoe vortex system. Upstream of the hemisphere this horseshoe vortex system dominates. The stagnation area is located close to the lower front surface of the hemisphere. The flow is accelerated along the contour of the hemisphere. At the apex of the hemisphere the flow detaches. As a consequence of the flow separation a shear layer and a recirculation area appear. The latter is separated from the outer field by a dividing streamline. Strong shear layer vorticity can be observed leading to the production of Kelvin-Helmholtz vortices which travel downstream in the flow field. In the reattachment region the flow impinges on the wall and a splatting effect occurs, redistributing momentum from the wall-normal direction to the streamwise and spanwise directions.

To compare the experimental and numerical results a time-averaging of the flow is carried out. The laser-Doppler anemometry (LDA) measurements are averaged over a long time period of about 1370 dimensionless time units (based on U_∞ and D), whereas the LES results are averaged over a shorter period of approximately 90 dimensionless time units which is still sufficient. The present study focuses on the detailed view of the time-averaged velocity field and the associated time-averaged Reynolds stresses in the symmetry plane.

Figure 1 presents the comparison of the LDA measurements and the LES predictions. First, the oncoming flow upstream of the hemisphere in the region $1.5 \leq x/D \leq 0.75$, is analyzed. The experimental results show that the thickness of the approaching boundary layer is matching the height of the hemisphere well with $z/D \approx 0.5$. A comparable velocity distribution is visible in the LES. The size of the horseshoe vortex system directly depends on the turbulence intensity of the approaching flow (see Wood et al., 2016): The higher the turbulence intensity is, the smaller the vortex system is. Comparing Fig. 1(g) with 1(h) highlights that the LES prediction relying on the STIG data leads to a close agreement of the streamwise velocity fluctuations with the LDA data in this region. Consequently, the horseshoe vortex system computed by LES fits well to the experiment (see Figs. 1(c) and 1(d)). A rough estimation of the detachment point position yields $x/D \approx -1.0$ in the measurements. In the simulation on the medium grid the detachment point is found at about $x/D = -0.85$. As explained in Wood et al. (2016) the horseshoe vortex system is composed of pairs of counter-rotating vortices. In the LES prediction one vortex pair is visible in Fig. 1(b), whereas in the measurements the near-wall resolution was insufficient to resolve these structures The position of the stagnation point ($\Theta_{LES}^{STAG} = 160°$) also agrees quite well with the experimental reference value of $\Theta_{EXP}^{STAG} = 166°$). A good agreement is also achieved in the next region, the acceleration area. Another interesting location is the separation point on the surface of the hemisphere. It marks an important characteristic for the validation of numerical simulations. Its position depends on various influence parameters (Reynolds number, turbulence intensity of the boundary layer and surface roughness). The predicted flow detaches at an angle of $\Theta_{LES}^{SEP} = 88°$, which is comparable to the LDA measurements ($\Theta_{EXP}^{SEP} \approx 90°$). The separated flow evolves into a free shear layer. This phenomenon can be observed as a strong velocity gradient between the outer flow field and the recirculation area in the wake. As expected the largest Reynolds stresses (normal and shear stresses) are found in the free shear layer and a close agreement is observed between the measured and predicted data. The size of the recirculation area can be evaluated based on the reattachment point of the time-averaged flow in the symmetry plane. The measurements provide a value of $x_{EXP}^{reattach}/D \approx 1.04$, whereas the LES predicts a slightly too long recirculation area of $x_{LES}^{reattach}/D = 1.18$. These minor differences in the length of the recirculation area between experimental and numerical results is due to the slightly different separation angles mentioned above. Overall a close agreement is found between the LDA data and the predicted LES results on the medium

grid. These numerical data on the medium grid also match very well with the predictions on the fine grid (De Nayer et al., 2016) available on the ERCOFTAC Knowledge Base Wiki under http://qnet-ercoftac.cfms.org.uk/w/index.php/UFR_3-33.

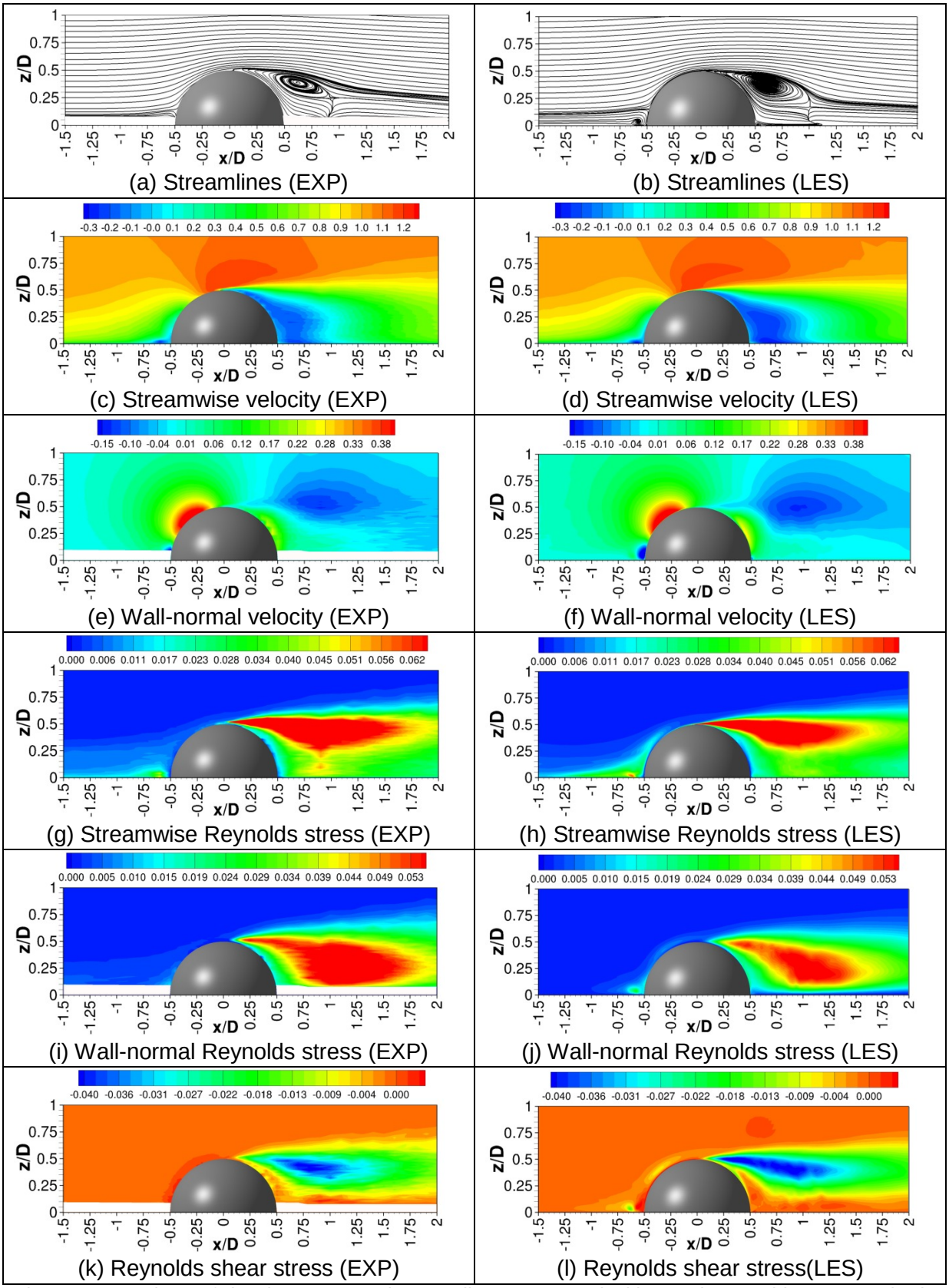

Fig. 1: Comparison of the time-averaged streamlines, mean velocities and Reynolds stresses in the symmetry plane: LDA measurements (left) and LES predictions (right).

Prediction of the Flow past the Flexible Hemisphere

After validating the LES prediction on the medium grid based on the experimental data and the corresponding simulations on the fine grid (Wood et al., 2016; De Nayer et al., 2016), the next step is to tackle the coupled FSI problem. Thus, the rigid hemisphere is replaced by the membranous structure and the computational methodology is extended by the CSD simulation and the coupling scheme described above. At the beginning of the coupled simulation the fluid flow is initialized by a pure LES and the structure is defined by a factor of ten times higher Young's modulus to avoid divergence of the coupling scheme. Then, the Young's modulus is slowly decreased again to the original value during the first 5000 time steps.
Figure 2 depicts first results for the coupled simulation after these initialization steps when the system is fully developed. The time series starts at an arbitrarily chosen instant in time and shows 12 different states with a temporal resolution of 3 ms covering a time interval of about one flow-over time of the hemisphere. The figures show the pressure distribution on the membrane and the magnified deformations of the surface. Since the overall deformations are small at the present Reynolds number investigated, a magnification factor of 15 is applied here. Obviously, the largest deformations are found at the stagnation region of the hemisphere, where the largest pressure is observed similar to the rigid case (Θ_{LES}^{STAG} = 160°). However, due to the oncoming turbulence generated in the present simulation by the synthetic inflow generator applied in the source term formulation (Schmidt and Breuer, 2016) already in this region strong fluctuations of the pressure and thus also of the deformations are visible. The acceleration of the flow around the hemisphere leads to a pressure minimum which is visible on the structure as an arch like structure, which intersects the x-z symmetry plane shortly before the apex of the structure. This can be recognized in all snapshots, but is superimposed by fluctuations of the pressure field. Clearly visible are strong deformations on the leeward side of the hemispherical obstacle. Animations of these deformations indicate wave-like deformations of the structure which are generated already at the windward side of the structure or near the circumference and are then transported in downstream direction. This is a first hint that these deformations are the results of the strong shear layer vorticity observed past the separation line leading to the generation of Kelvin-Helmholtz vortices. These vortices travel downstream in the flow field and interact with the flexible structure. However, in case of the rigid hemisphere a second “von Kàrmàn”-shedding process from the lateral sides of the hemisphere was also observed in the wake of the obstacle at a lower frequency (Wood et al., 2016). This second shedding process involves an interesting pattern of two clearly distinguishable types that switch in shape and time. Either alternating or symmetric shedding of large vortices was detected in the wake. Assuming that similar phenomena can also be found in case of the flow past the flexible hemisphere, these flow structures are expected to significantly affect the deformation of the membrane.
In the ongoing work these deformations will be analyzed in more detail taking the frequency spectra into account. The task will be to detect characteristic oscillations of the structure and to compare the corresponding frequencies on the one hand to those frequencies found in the flow around the rigid hemisphere (i.e., 7.9 Hz ≤ f_1 ≤ 10.6 Hz for shear layer vortices and f_2 = 5.5 Hz for von Kàrmàn shedding process, see Wood et al., 2016) and on the other hand to the first 15 eigenfrequencies of the structure found in the range 30 Hz ≤ $f_{membrane}$ ≤ 60 Hz.

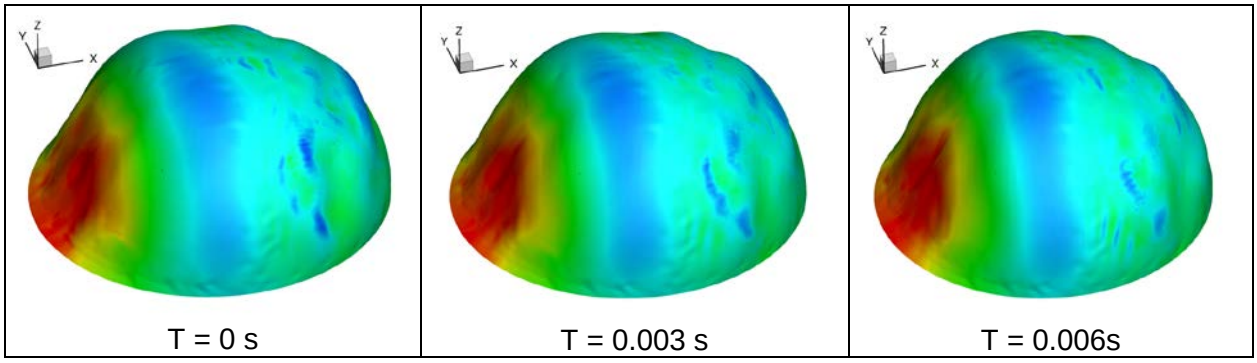

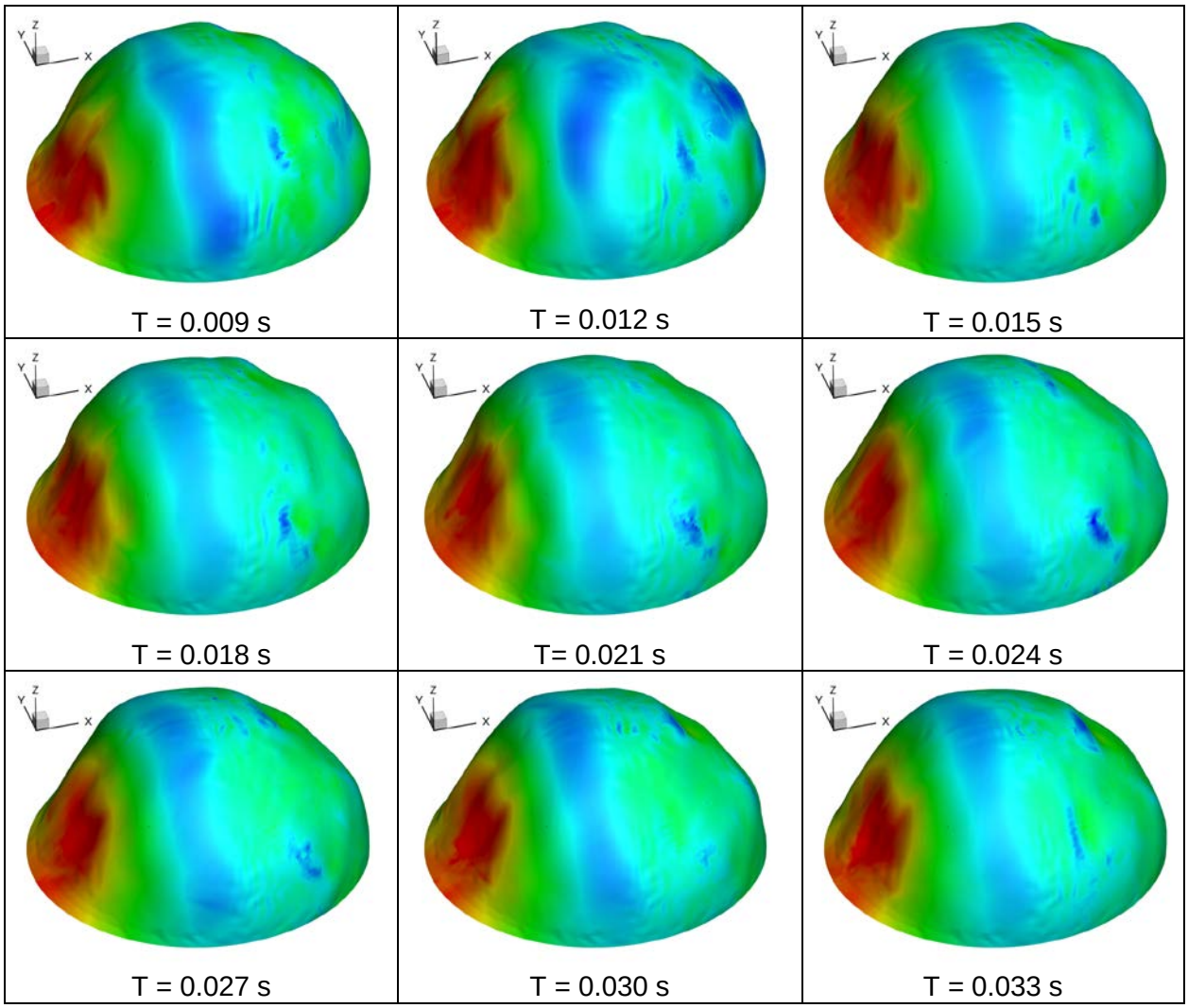

Fig. 2: History of the deformation of the membranous structure (magnification factor = 15) and distribution of the pressure on the hemisphere.

Conclusions

A complementary experimental-numerical investigation is carried out on the coupled FSI problem of the flow past a thin-walled hemispherical membranous structure placed in a thick boundary layer. The entire study is split up in subsequent steps of increasing complexity. First, the rigid case was analyzed in detail based on LDA measurements and LES predictions of extremely refined grids. The outcome published in Wood et al. (2016) and De Nayer et al. (2016) showed a close agreement between the measurements and the prediction providing confidence in the entire experimental and numerical methodology and especially in the generation of appropriate inflow conditions. In order to allow LES predictions on a coarser grid and thus to save an enormous amount of CPU-time for the even more resource demanding coupled simulations, simulations on a medium grid were carried out in a second step. The results still show a close agreement with the measurement data. In a third step, first coupled simulations are carried out. The preliminary results of the simulation show reasonable instantaneous deformations of the membrane which are presently analyzed according to their physical properties such as characteristic amplitudes and spectral content.
In the experimental counterpart at the same time additional PIV measurements of the flow field and digital-image correlation measurements of the displacements of the membrane ex-

posed to the turbulent boundary layer are performed (see **part I** of this contribution). The results of both approaches will be thoroughly compared in the near future similar to the analysis carried out for the flow past the rigid hemisphere.

Acknowledgements

The numerical part of the project is financially supported by the Deutsche Forschungsgemeinschaft under the contract number BR 1847/12-2. The computations were carried out on SuperMUC at LRZ Munich under the contract number pr84na.

References

Bletzinger, K.-U., Wüchner, R., Kupzok, A., 2006: "Algorithmic treatment of shells and free form-membranes in FSI". In: Bungartz, H.-J., Schäfer, M. (Eds.), Fluid-Structure Interaction, Lecture Notes in Computational Science and Engineering, LNCSE, vol. 53. Springer, Heidelberg, pp. 336-355.
Breuer, M., 2002: "Direkte Numerische Simulation und Large-Eddy Simulation turbulenter Strömungen auf Hochleistungsrechnern", Habilitationsschrift, Universität Erlangen-Nürnberg, Berichte aus der Strömungstechnik, Shaker Verlag, Aachen, Germany.
Breuer, M., De Nayer, G., Münsch, M., Gallinger, T., Wüchner, R., 2012: "Fluid-structure interaction using a partitioned coupled predictor-corrector scheme for the application of large-eddy simulation", J. Fluids Structures 29:107-130.
De Nayer, G., Kalmbach, A., Breuer, M., Sicklinger, S., Wüchner, R., 2014: "Flow past a cylinder with a flexible splitter plate: A complementary experimental-numerical investigation and a new FSI test case (FSI-PfS-1a) ", Computers and Fluids 99:18-43.
De Nayer, G., Breuer, M., 2014: "Numerical FSI investigation based on LES: Flow past a cylinder with a flexible splitter plate involving large deformations (FSI-PfS-2a)", Int. J. Heat Fluid Flow 50:300-315.
De Nayer, G., Schmidt, S., Wood, J.N., Breuer, M., 2016: „Investigations on the flow past a wall-mounted hemisphere based on LES and synthetically generated turbulence", 11th Int. ERCOFTAC Symp. on Eng. Turb. Modelling and Measurements, ETMM–11, Palermo, Sicily, Sept. 21–23, 2016.
Fischer, M., Firl, M., Masching, H., Bletzinger, K.-U., 2010: "Optimization of non-linear structures based on object-oriented parallel programming". In: Topping et al. (Eds.), Seventh Int. Conf. Eng. Comput. Technology, ECT2010. Civil-Comp Press, Stirlingshire, UK, p. 67.
Klein, M., Sadiki, A., Janicka, J., 2003: "A digital filter based generation of inflow data for spatially-developing direct numerical or large-eddy simulations", J. Comput. Phys. 186:652-665.
Rhie, C.M., Chow, W.L., 1983: "Numerical study of the turbulent flow past an airfoil with trailing edge separation". AIAA J. 21 (11):1525-1532.
Savory E., Toy N., 1986: "Hemisphere and hemisphere-cylinders in turbulent boundary layers", J. Wind Engineering and Industrial Aerodynamics 23:345-364.
Schmidt S., Breuer M., 2016: "Source term based synthetic turbulence inflow generator for eddy-resolving predictions of an airfoil flow including a laminar separation bubble", submitted.
Sicklinger, S., Belsky, V., Engelmann, B., Elmqvist, H., Olsson, H., Wüchner, R., Bletzinger, K.-U., 2014: "Interface Jacobian based co-simulation", Int. J. Numer. Meth. Eng., 98:418-444.
Smagorinsky, J., 1963: "General circulation experiments with the primitive equations I: The basic experiment". Mon. Weather Rev. 91 (3):99-165.
Wang, T., Wüchner, R., Sicklinger, S., Bletzinger, K.-U., 2016: "Assessment and improvement of mapping algorithms for non-matching meshes and geometries in computational FSI", Computational Mechanics 57 (5):793-816.
Wood, J.N., Breuer, M., 2015: "Towards FSI: LDA-investigations of the flow past a hemisphere in an artificially generated turbulent boundary layer", 23. Gala-Fachtagung Lasermethoden in der Strömungsmesstechnik", Sept. 8-10, 2015, TU Dresden, pp. 30-1–30-8, ISBN 978-3-9816764-1-9.
Wood, J.N., De Nayer, G., Schmidt, S., Breuer, M., 2016: "Experimental investigation and large-eddy simulation of the turbulent flow past a smooth and rigid hemisphere", Flow, Turbulence and Combustion 97(1):79-119.